

A model for dark matter, naturalness and a complete gauge unification

Kimmo Kainulainen^{a,c} Kimmo Tuominen^{b,c} Jussi Virkajärvi^{a,c}

^aDepartment of Physics, University of Jyväskylä,
P.O.Box 35 (YFL), FI-40014 University of Jyväskylä, Finland

^bDepartment of Physics, University of Helsinki,
P.O.Box 64, FI-00014 University of Helsinki, Finland

^cHelsinki Institute of Physics,
P.O. Box 64, FI-00014 University of Helsinki, Finland

E-mail: kimmo.kainulainen@jyu.fi, kimmo.i.tuominen@helsinki.fi,
jussi.virkajarvi@jyu.fi

Abstract. We consider dark matter in a minimal extension of the Standard Model (SM) which breaks electroweak symmetry dynamically and leads to a complete unification of the SM and technicolor coupling constants. The unification scale is determined to be $M_U \approx 2.2 \times 10^{15}$ GeV and the unified coupling $\alpha_U \approx 0.0304$. Moreover, unification strongly suggest that the technicolor sector of the model *must* become strong at the scale of $\mathcal{O}(\text{TeV})$. The model also contains a tightly constrained sector of mixing neutral fields stabilized by a discrete symmetry. We find the lightest of these states can be DM with a mass in the range $m_{\text{DM}} \approx 30 - 800$ GeV. We find a large set of parameters that satisfy all available constraints from colliders and from dark matter search experiments. However, most of the available parameter space is within the reach of the next generation of DM search experiments. The model is also sensitive to a modest improvement in the measurement of the precision electroweak parameters.

Keywords: Dark matter, Naturality, Unification, Technicolor

Preprint: HIP-2015-12/TH

Contents

1	Introduction	1
2	General model of dark matter	3
2.1	Gauge interactions	3
2.2	Scalar interactions and masses	4
2.3	Rotation to the mass eigenbasis	5
2.4	Renormalizable and anomaly free implementation	6
3	Unification	7
3.1	Unification of the SM coupling constants	7
3.2	Unification of all couplings including $\alpha_4 \equiv \alpha_{TC}$	9
4	Experimental constraints on low energy theory	11
4.1	Results of a generic MCMC scan	14
4.2	Benchmark models	16
5	Additional bounds: Higgs to $\gamma\gamma$ and a light composite scalar	17
5.1	Higgs to $\gamma\gamma$	18
5.2	Dynamical Higgs boson mass scale	19
6	Conclusions	21

1 Introduction

In contrast with its celebrated finding of the Higgs boson [1, 2], LHC has so far failed to discover any obvious sign for new physics. Yet compelling evidence for new physics abound. For example the existence of a large dark matter component in the energy density of the universe is currently lacking a proper elementary particle physics context. Standard model is also plagued by the hierarchy problem, *i.e.* it lacks a natural explanation for the lightness of the Higgs particle. Finally, SM does not give rise to coupling constant unification, which would be highly desirable on theoretical grounds. Yet another issue is that Standard Model cannot explain why the universe contains only matter. Of these issues the DM problem is the most tangible one phenomenologically, and DM studies have indeed recently been the leading motivation for the construction and analyses of beyond SM scenarios.

Dark matter can of course be considered separately from the issues of hierarchy problem and unification. In particular scalar dark matter models have been very popular recently [3–10]. These models are attractive because of their simplicity and because of possible connection to a new, larger dark sector interacting with the SM through the Higgs portal. Alternatively one can require that the DM is a part of a larger, independently motivated particle physics model. In this class the leading paradigm until recently was supersymmetry (SUSY) and in particular the minimal supersymmetric standard model. SUSY is compelling for many reasons, which include theoretical connections to (super)string theory and supergravity. From the phenomenological point of view SUSY is attractive because it could provide a solution to all main issues mentioned above. However, no sign of SUSY has been found. Instead

the minimal supersymmetric standard model is getting ever more tightly constrained by the data.

Another popular model building paradigm involves new strong dynamics (technicolor) sourcing the electroweak symmetry breaking. The currently favored technicolor (TC) models are based on the idea of quasiconformality [11, 12], concrete realizations of which are the minimal and next to minimal walking technicolor models [13, 14]. Technicolor was originally put forward as a solution of the hierarchy problem. However, it was recently shown that TC models can easily also provide unification of SM gauge couplings [15–17] and they have also shown to contain several possible DM candidates [15, 16, 18–29].

In this paper we consider a model for particle DM, which is deeply motivated by the TC paradigm and by the requirement of the gauge coupling unification. Yet, the DM-sector of the model may be considered also independent of its TC context. Therefore we first discuss the generic low-energy setup featuring new leptons transforming as a doublet and a triplet under the weak gauge group, and their mixing patterns and couplings with the gauge fields and with a Higgs-like scalar sector. The setup naturally leads to a thermal relic DM candidate, completely external to the strongly interaction sector and with fully deterministic couplings with ordinary matter. We also discuss a concrete model for dynamical electroweak symmetry breaking, which determines all mass terms and effective Higgs couplings.

This model for dark matter was originally introduced in refs. [15, 16, 22, 28]. Here we modify the underlying implementation of the model and significantly extend the analysis of ref. [16] by inclusion of all latest observational constraints. We also study more closely some benchmark scenarios for which we perform a new MCMC scan of the parameter space. We also analyze new consistency constraints arising from LHC-bounds on invisible and radiative Higgs decays. We find that the model can provide a naturally stable DM particle with a mass in the range $m_{\text{DM}} \sim 30 - 800$ GeV. Most of the allowed parameter space is within the reach of the next generation of direct and indirect DM search experiments. Also electroweak precision data, especially the Peskin-Takeuchi S -parameter, provide stringent bounds on the model.

We also show that the model gives rise to perfect 1-loop unification of *all* gauge couplings, including also the new technicolor interaction. The common unification scale and coupling are accurately determined: $M_{\text{U}} \approx 2.2 \times 10^{15}$ GeV and $\alpha_{\text{U}} \approx 0.0304$. The unification of the technicolor coupling is very sensitive to, and hence accurately determines the TC 1-loop IR-pole: $\Lambda_{\text{TC}}^{1\text{-loop}} \approx 340$ GeV. Based on the QCD-analogue, this value strongly supports the natural TC scale $\Lambda_{\text{TC}} \approx 3$ TeV. This result provides an important check on the internal consistency of the model.

The paper is organized as follows: We briefly review the model in section 2 complete with determination of all gauge- and scalar couplings and the mass terms and a full implementation in the TC context. In section 3 we study the unification of the standard model and the technicolor gauge couplings. The dark matter analysis together with imposing laboratory constraints is described in section 4. Here we also show the results MCMC-scan of the model parameter space and show that our WIMP is compatible with all current observational constraints. In section 5 we consider the LHC constraints on higgs decays and radiative corrections to its mass. Finally in 6 we give our conclusions and outlook.

2 General model of dark matter

We consider a model where the dark matter candidate is a mixture between electroweak singlet and neutral components of electroweak doublet and triplet fermions. Such candidate arises from a low energy Lagrangian of the form

$$\mathcal{L}_{\text{GM}} = \mathcal{L}_{4f,g} + \mathcal{L}_{\text{Ad},g} + \mathcal{L}_{4f,H} + \mathcal{L}_{\text{Ad},H} + \mathcal{L}_{\text{SM}}, \quad (2.1)$$

where $\mathcal{L}_{4f,g}$ describes the gauge sector of heavy 4th lepton family and $\mathcal{L}_{\text{Ad},g}$ that of the SU(2) adjoint and singlet Weyl fermions and $\mathcal{L}_{4f,H}$ and $\mathcal{L}_{\text{Ad},H}$ detail their interactions with scalar fields. Finally \mathcal{L}_{SM} describes Standard Model, where Higgs may be either a fundamental or an effective doublet field. We will now briefly introduce the relevant terms in the Lagrangian following ref. [16].

2.1 Gauge interactions

We denote the left handed heavy doublet by $L_L = (N_L E_L)^T$ and the charged right handed singlet by E_R . Using the SM-like hypercharge assignments the kinetic and gauge interaction terms for these fields become equal to the corresponding terms in the SM:

$$\mathcal{L}_{4f,g} = i\bar{L}_L \not{\partial} L_L + i\bar{E}_R \not{\partial} E_R + \mathcal{L}_W + \mathcal{L}_Z + \mathcal{L}_A, \quad (2.2)$$

where the gauge currents are given by

$$\begin{aligned} \mathcal{L}_W &= \frac{g}{\sqrt{2}} (W_\mu^- \bar{E}_L \gamma^\mu N_L + W_\mu^+ \bar{N}_L \gamma^\mu E_L), \\ \mathcal{L}_Z &= \frac{g}{2c_W} Z_\mu (\bar{N}_L \gamma^\mu N_L + (2s_W^2 - 1) \bar{E}_L \gamma^\mu E_L + 2s_W^2 \bar{E}_R \gamma^\mu E_R), \\ \mathcal{L}_A &= -e A_\mu \bar{E} \gamma^\mu E, \end{aligned} \quad (2.3)$$

where g is the weak coupling constant and $c_W \equiv \cos \theta_W$ and $s_W \equiv \sin \theta_W$, where θ_W is the Weinberg angle.

The Lagrangian for the left handed SU(2) adjoint triplet $\omega = (w^1, w^3, w^3)$ and the right handed singlet β^\dagger Weyl fermions is

$$\mathcal{L}_{\text{Ad},g} = i\omega^\dagger \bar{\sigma}^\mu D_\mu \omega + i\beta \sigma^\mu \partial_\mu \beta^\dagger. \quad (2.4)$$

Here $\sigma^\mu \equiv (1, \vec{\sigma})$ and $\bar{\sigma}^\mu = \sigma_\mu$, where σ^i are the usual Pauli matrices, and the covariant derivative is $D_\mu^{ac} = \partial_\mu \delta^{ac} + g\epsilon^{abc} A_\mu^b$. We can go to the 4-component notation by defining charged Dirac spinors $w_D^- = (w_\alpha^- (w^+)^\dagger{}^\alpha)^T$ and $w_D^+ = (w_\alpha^+ (w^-)^\dagger{}^\alpha)^T$ and neutral Majorana spinors $w_M = (w_\alpha^3 (w^3)^\dagger{}^\alpha)^T$ and $\beta_M = (\beta_\alpha \beta^\dagger{}^\alpha)^T$, where $w^\pm = (w^1 \mp iw^2)/\sqrt{2}$ are the two-component charge eigenstates. In the 4-component notation the Lagrangian (2.4) becomes:

$$\begin{aligned} \mathcal{L}_{\text{Ad},g} &= i\bar{w}_D \not{\partial} w_D + \frac{i}{2} \bar{w}_M \not{\partial} w_M + \frac{i}{2} \bar{\beta}_M \not{\partial} \beta_M \\ &+ g (W_\mu^+ \bar{w}_M \gamma^\mu w_D + W_\mu^- \bar{w}_D \gamma^\mu w_M - W_\mu^3 \bar{w}_D \gamma^\mu w_D), \end{aligned} \quad (2.5)$$

where $w_D \equiv w_D^-$. Note that the neutral field w_M does not couple to neutral gauge boson, and that the singlet field β_M has no gauge couplings. This interaction pattern has important consequences for the observability of the DM particle in the model.

2.2 Scalar interactions and masses

The masses and mixings of the new fields introduced above are determined by their couplings with the scalar sector, which we represent by an effective SM-like Higgs doublet H . First, the gauge-invariant interactions between H and the 4th family leptons and the neutral singlet are, up to dimension five operators, given by:

$$\mathcal{L}_{4f,H} = y_E \bar{L}_L H E_R + y_\beta \bar{L}_L \tilde{H} \beta_R + \frac{\lambda_{\text{NN}}}{\Lambda} (\bar{L}_L \tilde{H}) (\tilde{H}^T L_L^c) + \text{h.c.}, \quad (2.6)$$

where $\tilde{H} = i\tau^2 H^*$ and y_E , y_β and λ_{NN} are dimensionless coupling constants and $\Lambda \gg v$ is yet some unknown scale related to the UV complete theory generating the full flavor structure of the model. After symmetry breaking the first Yukawa term generates a Dirac mass $m_E = y_E v / \sqrt{2}$ for the charged lepton E , where v is the vacuum expectation value of the neutral composite Higgs field h . Second Yukawa term and the non-renormalizable dimension five operator produce Dirac and Majorana mass terms for the neutrino mass matrix.

Note that all interactions in Eqs. (2.2), (2.5) and (2.6) are invariant under Z_2 symmetry transformation, where

$$E \rightarrow -E, \quad N \rightarrow -N, \quad \beta \rightarrow -\beta \quad \text{and} \quad w \rightarrow -w. \quad (2.7)$$

We take this to be an exact symmetry of the model, which then forbids any couplings between the SM particles and the doublet or triplet fields. This symmetry is crucial for the stability of the dark matter in the model. We next allow all couplings between H and the SU(2) adjoint fields, which are consistent with the Z_2 -symmetry, again up to dimension five operators:

$$\mathcal{L}_{\text{Ad},H} = y_w \tilde{H}^T \omega L_L + \frac{\lambda_{w\beta}}{\Lambda} \beta H^\dagger \omega H + \frac{\lambda_{ww}}{\Lambda} H^\dagger \omega \omega H + \text{h.c.}, \quad (2.8)$$

where $\omega \equiv \omega^a \tau^a$ and $\tau^a = \sigma^a / 2$ in terms of the Pauli matrices and the scale Λ is the same we introduced in Eq. (2.6). Finally, we include a gauge- and Z_2 symmetric interaction Lagrangian to provide a mass to the singlet field β ¹:

$$\mathcal{L}_{\beta S} = y_R S \beta \beta + \text{h.c.} \quad (2.9)$$

After symmetry breaking the interactions (2.6) and (2.8-2.9) give rise to a 3×3 mass matrix for the neutral Majorana particles N , w_M and β_M (we drop the index M from w_M and β_M here):

$$\mathcal{L}_{\text{mass}} = \frac{1}{2} (\bar{N}_R, \bar{w}_R, \bar{\beta}_R) \begin{pmatrix} M_{\text{NN}} & m_{Nw} & m_{N\beta} \\ m_{Nw} & M_{ww} & m_{w\beta} \\ m_{N\beta} & m_{w\beta} & M_{\beta\beta} \end{pmatrix} \begin{pmatrix} N_L \\ w_L \\ \beta_L \end{pmatrix} + \text{h.c.} \quad (2.10)$$

where $M_{\text{NN}} = \lambda_{\text{NN}} v^2 / \Lambda$, $M_{ww} = \lambda_{ww} v^2 / 4\Lambda$, $M_{\beta\beta} = \sqrt{2} y_R v_s$, $m_{Nw} \equiv y_w v / 2\sqrt{2}$, $m_{N\beta} = y_\beta v / \sqrt{2}$ and $m_{w\beta} = \lambda_{w\beta} v^2 / 2\Lambda$, where v_s is the VEV of the singlet field S . The lightest mass eigenstate of this mass matrix is stable by the Z_2 symmetry, and is thus identified as the DM particle. Finally note that the Majorana mass M_{ww} is simultaneously the mass of the charged adjoint field w_D .

¹We assume that the bare mass term for β is zero even in the absence of a protecting symmetry principle. Whether such symmetry exists is related to a broader issue concerning the underlying flavor physics yielding also the effective couplings between the scalars and fermions. This is an interesting topic which, however, is beyond the scope of the analysis carried out in this paper.

2.3 Rotation to the mass eigenbasis

The symmetric mass matrix appearing in Eq. (2.10) can be diagonalized by a unitary transformation $U^T M U = m$, such that the mass eigenvalues are $m_i \geq 0$. Using the notation $\Omega_L \equiv (N_L, w_L^0, \beta_L)^T$ Eq. (2.10) can then be written in the form

$$\mathcal{L}_{\text{mass}} = \frac{1}{2} \bar{\Omega}_R M \Omega_L + \frac{1}{2} \bar{\Omega}_L M^\dagger \Omega_R = \frac{1}{2} \bar{\chi} m \chi, \quad (2.11)$$

where m is the diagonal mass matrix with positive mass eigenvalues. The corresponding mass eigenstates are Majorana fields given by $\chi = \chi_L + \chi_R \equiv U^\dagger \Omega_L + U^T \Omega_R$. This relation can be immediately inverted to give $\Omega_L = U \chi_L$ and $\Omega_R = U^* \chi_R$. Using these relations and Eqs. (2.3) and (2.5) we then find the weak currents of the heavy leptons and the SU(2) adjoint fermions in the mass eigenbasis:

$$\mathcal{L}_{\text{Af}}^W = \frac{g}{\sqrt{2}} W_\mu^- \sum_i U_{1i} \bar{E}_L \gamma^\mu \chi_{iL} + \text{h.c.}, \quad (2.12)$$

$$\mathcal{L}_{\text{Af}}^Z = \frac{g}{2c_W} Z_\mu \left(\sum_i |U_{1i}|^2 \bar{\chi}_{iL} \gamma^\mu \chi_{iL} + \sum_{i>j} \bar{\chi}_i (iV_{ij} + A_{ij} \gamma^5) \gamma^\mu \chi_j \right), \quad (2.13)$$

$$\mathcal{L}_{\text{Ad}}^W = g W_\mu^- \sum_i \bar{w}_D (V_i + iA_i \gamma^5) \gamma^\mu \chi_i + \text{h.c.}, \quad (2.14)$$

where

$$V_{ij} = \Im(U_{1i}^* U_{1j}), \quad A_{ij} \equiv \Re(U_{1i}^* U_{1j}), \quad V_i \equiv \Re(U_{2i}) \quad \text{and} \quad A_i \equiv \Im(U_{2i}) \quad (2.15)$$

and U_{ij} are the elements of the diagonalizing matrix U . Similarly, from Eqs. (2.6), (2.8) and (2.9) we can find the Higgs interactions in the mass eigenbasis:

$$\mathcal{L}_{h\chi} = -\frac{gh}{2m_W} \sum_{i \leq j} \bar{\chi}_i (S_{ij} + P_{ij} \gamma^5) \chi_j - \frac{g^2 h^2}{4m_W^2} \sum_i \bar{\chi}_i (S_{ii}^2 + P_{ii}^2 \gamma^5) \chi_i + \dots \quad (2.16)$$

Here dots refer to terms which do not affect tree level matrix element calculations and m_W is W^\pm -boson mass. The various mixing angle and mass dependent coefficients are defined as

$$\begin{aligned} S_{ij} &= -m_{N\beta} A_{ij} + (\delta_{ij} - 2) M_{\beta\beta} D_{ij} + m_i \delta_{ij}, \\ P_{ij} &= -m_{N\beta} i V_{ij} - i(\delta_{ij} - 2) M_{\beta\beta} E_{ij}, \\ S_{ii}^2 &= -m_{N\beta} A_{ii} - \frac{1}{2} M_{\beta\beta} D_{ii} + \frac{1}{2} m_i, \\ P_{ii}^2 &= -m_{N\beta} i V_{ii} + \frac{i}{2} M_{\beta\beta} E_{ii}, \end{aligned} \quad (2.17)$$

where m_i is the i 'th mass eigenvalue. The projection factors V_{ij} and A_{ij} are as defined in Eq. (2.15) and

$$D_{ij} \equiv \Re(U_{3i} U_{3j}) \quad \text{and} \quad E_{ij} \equiv \Im(U_{3i} U_{3j}). \quad (2.18)$$

Equations (2.12-2.18) contain all information needed to calculate the WIMP interaction rates relevant for the relic density and direct detection analyses.

2.4 Renormalizable and anomaly free implementation

The dark matter model discussed above is not a consistent extension of the SM on its own as it suffers from quantum anomalies. However, the low energy Lagrangian (2.1) can be embedded *e.g.* into the context of a renormalizable, anomaly free TC model where electroweak symmetry is broken dynamically. One possible realisation is to take this to be the minimal walking TC, and this possibility was explored in ref. [16] (see also [15, 22, 28]). Here, to illustrate different possibilities, we consider an alternative realization. The complete list of new fields and their quantum number assignments is shown in table 1. In addition to the

	SU(3) _c	SU(2) _L	U(1) _Y	SU(N _{TC})	Z ₂
L_L	1	2	-1/2	1	-1
E_R^c	1	1	1	1	-1
ω	1	adj.	0	1	-1
β	1	1	0	1	-1
\tilde{g}	adj.	1	0	1	-1
Q_L	1	2	1/6	3	1
U_R^c	1	1	-2/3	3	1
D_R^c	1	1	1/3	3	1
η_1	1	1	0	3	-1
η_2	1	1	0	3	-1
\tilde{G}	1	1	0	adj.	-1

Table 1. The table shows the new states added to SM, and their charge assignments under the SM gauge group and the technicolor gauge group which we will consider to be SU(3). Also shown is the discrete matter parity which is even for the SM matter fields.

fields introduced earlier (L_L , E_R^c , ω and β), the table shows the new strongly coupled sector responsible for the electroweak symmetry breaking. Of the new fermion fields, the techni-quarks Q_L , U_R^c , D_R^c , η_1 and η_2 , are gauged under a new vectorial gauge interaction SU(N_{TC}). We set $N_{TC}=3$. These elementary fermions form composite fields similar to the mesons and hadrons in QCD. We assume that only one doublet of the technifermions is gauged under the electroweak symmetry, while the remaining two Weyl fermions (η_1 and η_2) are singlet under all SM charges. We assume that similarly to other SM-singlet fermions also η_1 and η_2 are odd under the "matter parity" Z_2 . Finally, there are two Weyl fermions, \tilde{g} and \tilde{G} , transforming in the adjoint representation of SU(3) of QCD and TC, respectively². Both of these fields are assumed to be heavy and decoupled from low energy particle spectrum. These field are relevant neither for the dynamical symmetry breaking nor for the dark matter. However, as we will discuss in the next section, when \tilde{g} and \tilde{G} are included, along with the SU(2)-adjoint field ω , the model also gives rise to excellent gauge coupling unification.

At high energies the technicolor sector is described by the Lagrangian

$$\mathcal{L}_{TC} = -\frac{1}{4}F_{\mu\nu}^a F^{a\mu\nu} - \bar{Q}_L i \not{D}_L Q_L - \bar{U}_R i \not{D}_R U_R - \bar{D}_R i \not{D}_R D_R - \bar{\eta} i \not{D} \eta, \quad (2.19)$$

where $F_{\mu\nu}$ is the field strength of the technicolor gauge field and $Q = (U, D)^T$. The covariant derivative \tilde{D} contains only the technicolor gauge field while the covariant derivatives $D_{L,R}$ contain also the electroweak gauge fields. At low energies the strong dynamics is described

²For concreteness we have assigned the value $Z_2 = -1$ for these fields.

by an effective Lagrangian for composite mesons. Due to the different Z_2 parities of the techniquarks, the low energy composites are $\Sigma \sim \bar{Q}Q$ and $\sigma \sim \bar{\eta}\eta$. The former is the effective Higgs doublet which in our case is a composite field, and hence the model does not suffer from hierarchy problem. The field $\sigma \sim S + i\pi_s$ is another composite complex scalar, singlet under all SM charges.

The low energy effective Lagrangian is

$$\mathcal{L}_{\text{TC, eff}} = \text{Tr} D_\mu \Sigma^\dagger D^\mu \Sigma + \partial_\mu \sigma^\dagger \partial^\mu \sigma - V(\Sigma, \sigma), \quad (2.20)$$

where $\Sigma = (\zeta + i\vec{\pi} \cdot \vec{\sigma})/2$ is charged under the electroweak interactions (σ_i are the Pauli matrices) and

$$V(\Sigma, \sigma) = m^2 \text{tr} M^\dagger M + \lambda \text{tr} (M^\dagger M)^2 + \frac{1}{2} \mu_s^2 \pi_s^2, \quad (2.21)$$

where $M = \Sigma \oplus \sigma$. The real part, S , is identified with the field introduced in Eq. (2.9) to provide mass to the fermion field β , while for the pseudoscalar component π_s we have included an explicit mass term in Eq. (2.21). Even if the field π_s is light with respect to the intrinsic scale Λ_{TC} , it can be heavy with respect to the masses in the dark matter sector. If μ_s was comparable to, or smaller than the fermionic DM mass, the dark sector of the model would be more complicated, containing both fermionic and bosonic components. While this is an interesting possibility, we shall here assume that π_s is heavy and consequently the DM is purely fermionic. A mass term for π_s is expected to arise from the flavor physics providing the masses of SM matter fermions, and their origin can be accounted for by gauge dynamics (as in extended TC models).

As a final remark, we note that with the above particle content the TC sector might be close to conformality [30]. However, coupling between the TC sector and the SM fields via the gauge and Yukawa interactions will move the theory away from the conformal window [31–33]. Therefore, we will assume the properties of the TC sector to be QCD-like.

3 Unification

3.1 Unification of the SM coupling constants

For completeness we will first briefly review the argument for the unification of the SM coupling constants. More details can be found in ref. [15]. At one-loop the coupling constant α_n of an $\text{SU}(n)$ gauge theory is given by

$$\alpha_n^{-1}(\mu) = \alpha_n^{-1}(M_Z) - \frac{b_n}{2\pi} \ln \left(\frac{\mu}{M_Z} \right). \quad (3.1)$$

The beta function coefficient b_n is:

$$b_n = \frac{2}{3} T(R) N_{wf} + \frac{1}{3} T(R') N_{cb} - \frac{11}{3} C_2(G), \quad (3.2)$$

where $T(R)$ and $T(R')$ are the Casimirs of the representation R for N_{wf} Weyl fermions and of the representation R' for N_{cb} complex scalars and $C_2(G)$ is the quadratic Casimir of the adjoint representation of the gauge group. For SM we have three coupling constants corresponding to $n = 3, 2, 1$. Requiring that SM coupling constants unify means that the three couplings are all equal at some scale M_U : $\alpha_3(M_U) = \alpha_2(M_U) = \alpha_1(M_U)$ with $\alpha_1 = \alpha/(c^2 \cos^2 \theta_W)$ and $\alpha_2 = \alpha/\sin^2 \theta_W$, where c is a normalization constant that depends on the

choice of the unifying group. Here we shall use $c = \sqrt{3/5}$, corresponding to the SM matter unified into SU(5).

Using Eq. (3.1) we can now derive the following relation:

$$B \equiv \frac{b_3 - b_2}{b_2 - b_1} = \frac{\alpha/\alpha_3 - \sin^2 \theta_W}{(1 + c^2) \sin^2 \theta_W - c^2} = 0.721 \pm 0.004, \quad (3.3)$$

where the Weinberg angle θ_W and weak and strong coupling constants were evaluated at the Z -mass scale, using values from ref. [34]: $\sin^2 \theta_W(M_Z) = 0.23126 \pm 0.00005$, $\alpha^{-1}(M_Z) = 127.940 \pm 0.014$, $\alpha_3(M_Z) = 0.1193 \pm 0.0016$ and $M_Z = 91.1876 \pm 0.0021$ GeV.

The hypercharge assignment of our model renders the Technicolor sector identical to one extra SM generation from the electroweak interaction viewpoint. In addition we have one strongly interacting adjoint Weyl fermion, which affects the running of the QCD coupling and one weak triplet affecting the running of α_2 . The group factors are $T(R) = 1/2$ for the fundamental representation, $T(G) = n$ for the adjoint SU(N)-representation and $T(R) = c^2 Y^2 = (3/5)Y^2$ for the $U(1)_Y$ hypercharge gauge group. With N_g generations of ordinary fermions we then find:

$$\begin{aligned} b_1 &= \frac{4}{3}N_g + \frac{4}{3} = b_1^{\text{SM}} + \frac{37}{30} \\ b_2 &= \frac{4}{3}N_g - \frac{14}{3} = b_3^{\text{SM}} + \frac{5}{2} \\ b_3 &= \frac{4}{3}N_g - 9 = b_3^{\text{SM}} + 2. \end{aligned} \quad (3.4)$$

Note that the differences $b_i - b_j$ are independent of N_g , because they can not be affected by states forming complete representations of the unifying gauge group [35]. It is now clear that the SM does not unify since $B_{\text{theory}}^{\text{SM}} \simeq 0.53$. However in our model $B_{\text{theory}}^{\text{TC}} \simeq 0.722$, which is generously within one sigma of the extremely tight constraint (3.3). In fact the unification mass and coupling are very precisely determined by the coupling constant unification. If we define a chi-squared function

$$\chi^2(M_U, \alpha_U) \equiv \sum_{i=1}^3 \frac{(\alpha_i(M_U) - \alpha_U)^2}{\Delta\alpha_i^2}, \quad (3.5)$$

where $\Delta\alpha_i$ are the observational errors for each coupling given above in the text (these errors propagate essentially as such to the unification scale), we find that at 1σ -level:

$$M_U = (2.20 \pm 0.03) \times 10^{15} \text{ GeV}, \quad \text{and} \quad \alpha_U = 0.03042 \pm 0.00002. \quad (3.6)$$

In any grand unified theory nucleons are expected to decay via the exchange of gauge bosons with GUT scale masses. Schematically the partial decay width of the proton into a generic channel containing a meson and a lepton is

$$\Gamma = \gamma_{\text{QCD}}\gamma_{\text{GUT}}, \quad (3.7)$$

where γ_{GUT} contains the details of the underlying unified theory and γ_{QCD} contains the QCD parameters and the effective low energy constants parametrizing the hadronic matrix element relevant for the decay in question. For example, for a simple decay mode via a massive gauge boson exchange, assuming $M \approx M_U$, $\gamma_{\text{GUT}} \sim \alpha_U^2/M_U^4$. The precise details of course depend on the particular GUT model. We do not pursue such model building here; see e.g. [36, 37].

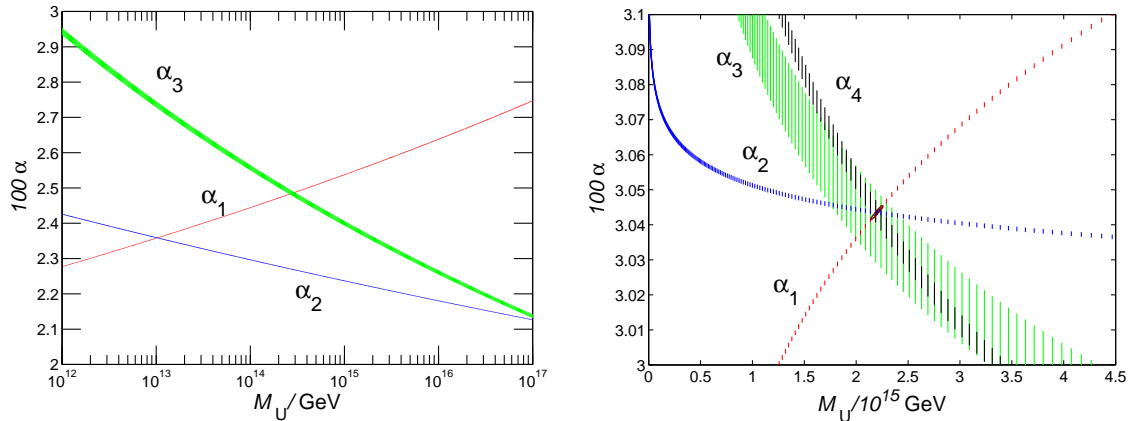


Figure 1. Left: the running of the gauge couplings in the SM. Note the logarithmic scale. Left: the running of all four couplings in the MWTC-DM model under consideration, including the TC-coupling α_4 . The ellipses show the 1- and 2- σ contours for unification scale and the unified coupling derived from the χ^2 -distribution (3.5). For the TC-coupling α_4 we took $331 \text{ GeV} < \Lambda_{\text{TC}}^{1\text{-loop}} < 351 \text{ GeV}$. Note the linear scale on the latter plot.

To obtain a parametric estimate, consider

$$\tau_N = \frac{1}{\Gamma} \sim \frac{f_\pi^2}{m_N} \frac{M_U^4}{\alpha_U^2 \alpha_N^2}, \quad (3.8)$$

where $f_\pi = 0.131 \text{ GeV}$, m_N is the mass of the nucleon and α_N the hadronic low energy constant. This must be determined from the lattice [38] and is subject to relatively large uncertainties [39, 40]; for $p \rightarrow e^+ \pi^0$ the estimates for the value of α_N range from 0.003 GeV^3 to 0.03 GeV^3 [39]. Using the value 0.01 GeV^3 compatible with the lattice calculation [39] and numbers from Eq. (3.6) results in $\tau_N \sim 10^{35} \text{ y}$, which is compatible with the current bound from the Super-Kamiokande $\tau_N > 10^{34} \text{ y}$ [34].

We plot the running couplings in figure 1 for the SM (left panel) and for the current model (right). The latter plot was created with linear M_U scale and zoomed to the unification coupling to reveal the almost perfect one-loop unification in our model. The tight error bars on the unification mass and the unified coupling can be used to make a formally accurate prediction for the value of the QCD-coupling at electroweak scale. Running the QCD-coupling backwards from the unification scale gives:

$$\alpha_3(M_Z) = 0.1120 \pm 0.0003, \quad (3.9)$$

which is consistent with but much tighter than the current observational limits³.

3.2 Unification of all couplings including $\alpha_4 \equiv \alpha_{\text{TC}}$

Above we considered only the unification of the SM coupling constants. In our model we have an additional gauge coupling related to the strong Technicolor interactions and it would

³Note that the running of the SM couplings will be affected by the strongly coupled TC sector at the scales below $\mathcal{O}(\text{TeV})$: the composite spectrum of technihadrons charged under the electroweak interactions will feed into the evolution and may affect the precision of the above result.

be more satisfying to have a unification of all four coupling constants. We now show that this indeed quite naturally takes place in our model.⁴

With the current particle content, shown in Table 1 we have:

$$b_4 = (4 + 2) \times \frac{1}{3} + 2 - 11 = -7. \quad (3.10)$$

Let us now require that α_2 and α_4 unify at M_U . This implies that:

$$C \equiv \frac{\sin^2 \theta_W - \alpha/\alpha_4}{c^2 - (1 + c^2) \sin^2 \theta_W} = \frac{b_4 - b_2}{b_2 - b_1}. \quad (3.11)$$

Theoretically, the particle content of the model gives:

$$C_{\text{th}} = \frac{b_4 - b_2}{b_2 - b_1} \approx 1.0556. \quad (3.12)$$

The “experimental” value of C depends on $\Lambda_{\text{TC}}^{1\text{-loop}}$, defined as the scale at which the inverse 1-loop coupling vanishes: $\alpha_4^{-1}(\Lambda_{\text{TC}}^{1\text{-loop}}) \equiv 0$. Using $\Lambda_{\text{TC}}^{1\text{-loop}} = M_Z$ gives $C_{\text{exp}}^{M_Z} \approx 1.0055 \pm 0.0006$, which is formally about 90 sigma’s away from the theoretical value. Since $C_{\text{exp}}^{M_Z} < C_{\text{th}}$ and b_4 is negative, the problem is that α_4 *undershoots* the unification value. We can improve the situation either by adding new fermion or boson fields to the particle spectrum to achieve a slower running, or by use of a larger $\Lambda_{\text{TC}}^{1\text{-loop}}$ to get an effectively positive $\alpha_4^{-1}(M_Z)$ initially in Eq. (3.11). Let us consider the latter option. From Eqs.(3.11-3.12) it is easy to see that the scale $\Lambda_{\text{TC}}^{1\text{-loop}}$ needed to achieve unification between α_4 and α_2 is given by:

$$-\frac{\alpha b_4}{2\pi} \log \frac{\Lambda_{\text{TC}}^{1\text{-loop}}}{M_Z} = [C_{\text{th}} - C_{\text{exp}}^{M_Z}] (c^2 - (1 + c^2) \sin^2 \theta_W). \quad (3.13)$$

Using the experimental input values for couplings and for the above computed values for C_{th} and $C_{\text{exp}}^{M_Z}$, propagating all errors throughout, we find:

$$\Lambda_{\text{TC}}^{1\text{-loop}} = 341 \pm 5 \text{ GeV}. \quad (3.14)$$

The right panel of figure 1 illustrates how the complete 4-coupling constant unification takes place at the scale and the coupling given by Eq. (3.6), when $\Lambda_{\text{TC}}^{1\text{-loop}}$ is chosen according to Eq. (3.14). Of course the energy scale where TC dynamics becomes strong is above the scale $\Lambda_{\text{TC}}^{1\text{-loop}}$ where the 1-loop coupling diverges. For example, for QCD itself, the simple 1-loop running Eq. (3.13), yields $\Lambda_{\text{QCD}}^{1\text{-loop}} \approx 57 \text{ MeV}$, while the typical scale for QCD is about an order of magnitude higher: $\Lambda_{\text{QCD}} \sim 700 \text{ MeV}$. If this holds also for TC, then the unification condition Eq. (3.14) predicts that

$$\Lambda_{\text{TC}} \sim 3 \text{ TeV}. \quad (3.15)$$

This agrees very well with what one would naively expect: if we write $\Lambda_{\text{TC}} \approx 4\pi F_\pi$, where F_π is the technipion decay constant, then the unification condition (3.15) sets $F_\pi \approx 250 \text{ GeV}$.

Even though such scalings are simply naive dimensional analysis, it is encouraging that unification of all couplings is not only possible in the model, but also determines the

⁴The results are dependent on the normalization of the hypercharge, i.e. the factor c . In principle its value is determined by the particle content and the structure of the unifying algebra; we assume the value $c = \sqrt{3/5}$ throughout here.

dynamical symmetry breaking to occur at the TeV scale. Even if our analysis is complete at 1-loop level, the results must be taken with a grain of salt: detailed results may be modified by higher order corrections and by threshold effects. Moreover, we have not addressed the underlying nature of flavor dynamics which gives rise to the couplings between the effective scalars and fermion fields, as this dynamics is decoupled from the other gauge interactions at 1-loop level. As an initial exploration of this model, our results nevertheless provide an interesting benchmark scenario for more detailed investigations in the future.

4 Experimental constraints on low energy theory

At low energies our model is parametrized by seven dimensionless couplings $y_E, y_\beta, y_w, y_R, \lambda_{\text{NN}}, \lambda_{ww}, \lambda_{w\beta}$ and three scales v, v_s and Λ . From these one can easily work out the entries in the mass matrix Eq. (2.10) of neutral fields and the mass of the new charged state E . From naive dimensional analysis we infer that $y_i < 4\pi$ and $\lambda_{ij} < (4\pi)^2$. Furthermore, assuming $v_s \sim v = 246$ GeV and $\Lambda \sim \mathcal{O}(\text{TeV})$, we find it reasonable to adopt the following prior ranges for the Lagrangian masses:

$$|M_{ij}| \leq 3000 \text{ GeV}; \quad |m_{ij}| \leq 2000 \text{ GeV} \quad \text{and} \quad 200 \text{ GeV} \leq m_E \leq 2000 \text{ GeV}. \quad (4.1)$$

We scanned this parameter range using Monte Carlo Markov Chain (MCMC) methods [16]. For each set of input parameters we diagonalize the DM mass matrix numerically, find the mass eigenvalues m_i and the diagonalizing matrix U_{ij} and identify the lightest eigenstate as the WIMP. We then check that the WIMP is stable, *i.e.* that it is the lightest of all states transforming nontrivially under the Z_2 symmetry.

The data shown in our result figures is compatible with the experimental and observational constraints from oblique electroweak precision data, the Z -boson and Higgs boson invisible decay width limits, cross section constraints from DM direct detection LUX, XENON100 and PICO experiments as well as DM indirect detection constraints from Ice-Cube, Super-Kamiokande and FERMI-LAT telescopes and from the AMS-02 experiment. For the data passing these tests, the DM relic density is calculated numerically and checked to be consistent with the most recent observations [41].

We do not require that our model provides the total observed abundance of the DM, inferred from the most recent CMB observations: $\Omega_{\text{DM}} h^2 = 0.1193 (\pm 0.0014)$ [41]. Instead, we impose this as an upper bound and compute how large a fraction of the total DM-density each parameter set is able to produce, defined as $f_{\text{rel}} \equiv \Omega_\chi h^2 / \Omega_{\text{DM}} h^2$. We accept models also with subleading DM in the interval:

$$0.05 \leq f_{\text{rel}} \leq 1.01. \quad (4.2)$$

This criterion affects the direct and indirect DM search constraints on WIMP-nucleon cross sections, which usually are given assuming that $f_{\text{rel}} = 1$. However, as long as different DM-components are weakly interacting, they all cluster roughly the same way, and a given subleading DM should make up only a fraction f_{rel} of the DM density in all cosmological substructures. We then constrain such subleading WIMPs using a scaled effective cross section [8, 9]:

$$\sigma_{\text{SD,SI}}^{\text{eff}} \equiv f_{\text{rel}} \sigma_{\text{SD,SI}} < \sigma_{\text{bnd}}, \quad (4.3)$$

where σ_{SD} refers to spin-dependent and σ_{SI} to spin-independent channel and σ_{bnd} is the bound from a given experiment. We imposed direct search bounds from XENON100 [42],

LUX [43] and PICO [44], as well as the indirect search bounds from IceCube [45, 46] and Super-Kamiokande [47, 48]. For explicit expressions for cross sections and for more detailed discussion of the implementation of these constraints see [16]⁵. Both SI- and SD-constraints are relevant for our model in different regions of the parameter space. However, the SI-constraint is typically the stronger one. There are particular cases where our DM particle has essentially but a dominantly pseudo-scalar coupling to the Higgs boson. In such case the WIMP-nucleus interaction is momentum transfer dependent and strongly suppressed. These solutions may avoid detection by any of the DM search programs currently under construction.

The new doublet and adjoint SU(2) states in our model, as well as the new states in the TC sector are charged under SU(2) and hence contribute to oblique S and T -parameters [49]. Explicit expressions of these contributions can be found in the appendix of ref. [16]. Here we use the experimental constraints [34]:

$$S = 0.00 \pm 0.08, \quad \text{and} \quad T = 0.05 \pm 0.07. \quad (4.4)$$

which include a 90% correlation between S and T as given by [34]. There are many other bounds coming from collider experiments. First, there is a direct LEP-II-bound on any charged particle i coupling to Z -boson: $m_i \geq 104.5$ GeV. LHC mass limits, while not as straightforward to implement, are typically much stronger. In our analysis we have used conservative bounds

$$m_E, m_{\omega_D} > 500 \text{ GeV}. \quad (4.5)$$

The Z -boson invisible decay width imposes a constraint on any particle with $m < M_Z/2$. The current bound from LEP-II is $\Gamma(Z \rightarrow \text{inv.}) = (2.984 \pm 0.008)\Gamma(Z \rightarrow \bar{\nu}\nu)$ [50]. As the best fit value is already 2σ below the SM prediction, we allow at most one standard deviation from new physics, which implies a bound

$$\delta_Z \equiv |U_{1i}|^4 \left(1 - \frac{4m_i^2}{m_Z^2}\right)^{3/2} < 0.008. \quad (4.6)$$

This rules out any WIMP with $m_{\text{DM}} < m_Z/2$ and a significant N_L component. Furthermore, if the WIMP is lighter than $m_H/2$, then also Higgs could decay to a pair of WIMPs. The invisible Higgs branching fraction R_I is constrained to be [51–53]:

$$R_I \equiv \frac{\Gamma_{\text{H,DM}}}{\Gamma_{\text{H,DM}} + \Gamma_{\text{SM,tot}}} \lesssim 0.17, \quad (4.7)$$

where $\Gamma_{\text{SM,tot}}$ is the total Higgs decay width in the SM and $\Gamma_{\text{H,DM}} = (G_F m_H / 2\sqrt{2}\pi) (|S_{ii}|^2 \beta_i^3 + |P_{ii}|^2 \beta_i)$, where $\beta_i \equiv (1 - 4m_i^2/m_H^2)^{1/2}$ and the index i refers to the WIMP as the lightest of the mass eigenstates. The bound (4.7) assumes SM-like Higgs-gauge and Higgs-fermion couplings. It would be relaxed to $R_I < 0.26$, if one allows Higgs and SM gauge fields to have non-SM-like couplings to photons and gluons [53]. However, in our analysis we always use the stronger constraint (4.7).

⁵Here we have improved our analysis related to IceCube and Super-Kamiokande limits by taking the DM annihilation branching fractions to different channels into account when imposing the constraints. We use W^+W^- limits for annihilation channels W^+W^- , ZZ and Zh , and $\tau^+\tau^-$ and $b\bar{b}$ limits as they are, including proper branching fractions in all channels.

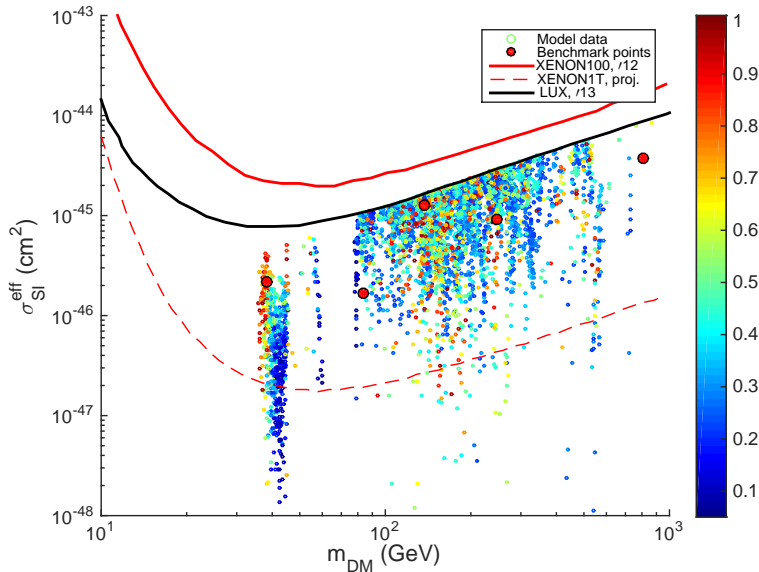


Figure 2. Scatter plot of the models passing all existing constraints as a function of the DM-mass and the predicted WIMP-nucleon SI-cross section. Colors represent the value of f_{rel} for each model as indicated by the bar on the right. Also shown are the current XENON100 [42], and LUX [43] limits as well as the predicted reach of the XENON1T experiment [54]. Large red dots show our five benchmark models.

Indirect observations are also sensitive on WIMPs annihilating in Galaxy center and in Galaxy halo. However, current limits on signals from neutrino detectors [55–57] are not stringent enough to be of use here. These annihilations could also create potentially observable flux of gamma-rays in the FERMI-LAT data [58–62]. However, our light WIMPs ($m_{\text{DM}} < m_W$) tend to annihilate to lighter fermions in a velocity suppressed p -wave via Z -boson resonance giving only a very weak gamma-ray signal. Thus, in our model the annihilation cross sections are below the current FERMI-LAT limits [58–62] in the most constrained low DM mass region. Only the FERMI-LAT limits from the Milky Way dwarf spheroidal satellite galaxies (dSphs) [63] are sensitive enough to constrain a small part of our model parameter space. In WIMP mass region $m_W \lesssim m_{\text{DM}} \lesssim 100$ GeV these limits [63] cut away a few points. For $m_{\text{DM}} \gtrsim 100$ GeV these limits have no impact. In all our results we show only data which passes these FERMI-LAT constraints. Finally, even though the annihilation cross section for subdominant DM in dSphs is larger than the canonical thermal relic cross section, the DM density is also expected to be smaller, scaled down by factor f_{rel} . This suppresses the flux of gamma-rays by a factor f_{rel}^2 making these constraints for subdominant DM even milder than for canonical thermal DM.

Finally, we imposed the constraints for DM annihilation cross section in the $b\bar{b}$ channel from ref. [64] (left panel Fig. 4), derived from the new AMS-02 [65] data on the secondary astrophysical antiproton to proton ratio. These limits cut away the few otherwise remaining points in the mass range $m_{\text{DM}} \sim 65 - 80$ GeV.

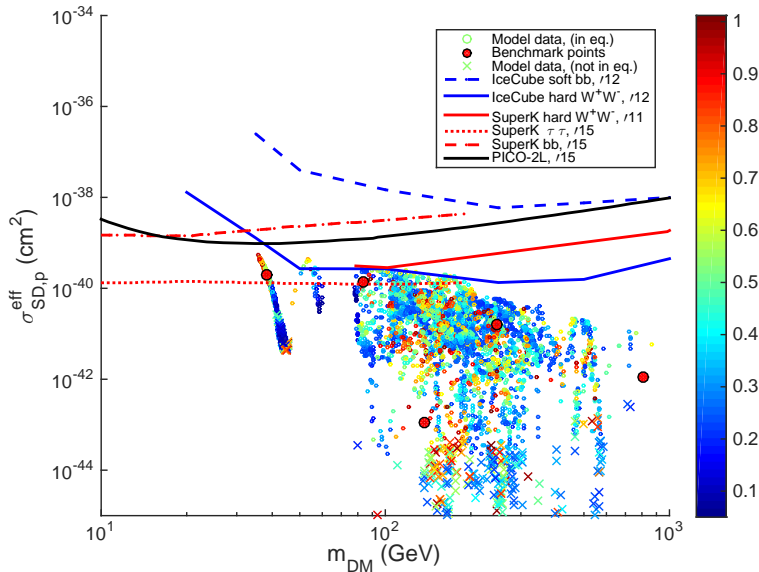


Figure 3. Scatter plot of the models passing all existing constraints as a function of the DM-mass and the WIMP-proton SD-cross section. Shown are also the best current constraints direct [44] (PICO) and indirect searches [45, 46] (ICECUBE) and [47, 48] (Super-Kamiokande). In models indicated with dots WIMPs would have reached equilibrium between capture and annihilations in the sun and the models indicated with crosses they have not. For more detailed treatment of the indirect observation channels see [16].

4.1 Results of a generic MCMC scan

In figure 2 we show the distribution of the models that passed all tests in our MCMC runs as a function of the DM-mass, the effective WIMP-nucleon SI-cross section and the relative relic abundance f_{rel} , whose value is indicated by the vertical bar to the right of the plot. The advantage of our using the effective cross section here is that one immediately sees how much a given direct search experiment needs to improve its sensitivity in order to rule out a given set of parameters. It is still easy to find acceptable models, in particular with a subleading DM. However, most of the allowed parameter space, including all our benchmark models to be defined below, is within the reach of the next round of the direct search experiments, which improve the current bound on $\sigma_{\text{SI}}^{\text{eff}}$ by a factor of ~ 50 .

Let us now very briefly explain the data in figure 2. When $m_{\text{DM}} \lesssim 80$ GeV, the DM particles annihilate into light SM fermions. A vertical cluster of points around $m_{\text{DM}} \approx 45$ GeV corresponds to the Z-boson resonance. Another, weaker cluster, around $m_{\text{DM}} \approx 60$ GeV (containing only blue points) corresponds to the Higgs boson resonance. Solutions at range $m_{\text{DM}} \sim 65 - 80$ GeV are excluded by AMS-02 constraints as was previously explained. For $m_{\text{DM}} \gtrsim 80$ GeV, new annihilation channels, first to W^-W^+ and then to ZZ , Zh , hh and $t\bar{t}$ open up sequentially and begin to dominate the cross section. None of these channels have equally striking signature as do the resonances.

In figure 3 we show the projection of accepted points as a function of the spin dependent interaction cross section $\sigma_{\text{SD,p}}^{\text{eff}}$ and the WIMP mass. It is evident that the existing SI-constraints are stronger than the SD-constraints. However, the IceCube and Super-

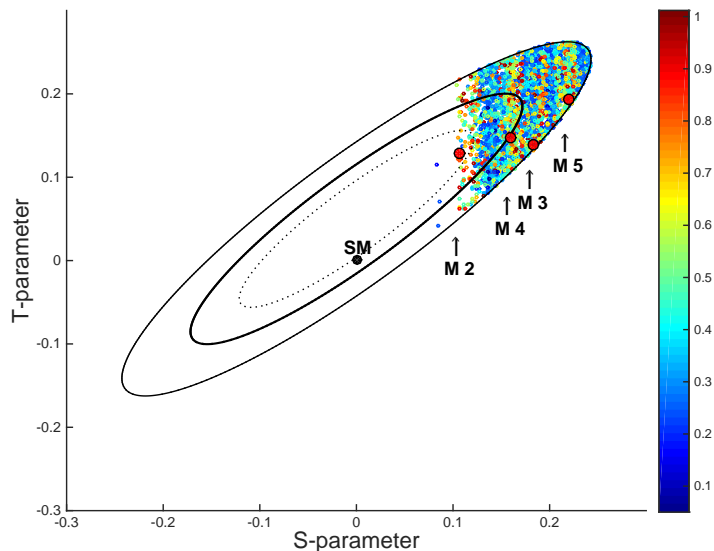


Figure 4. Scatter plot of the models passing all existing constraints in the plane of precision electroweak parameters S and T . The ellipses are the experimental 1σ , 1.6σ and 2.6σ confidence contours for S and T [34]. Note that the benchmark model 2 is as good a fit to the data as is the SM.

	M_{NN}	M_{ww}	$M_{\beta\beta}$	M_{Nw}	$M_{N\beta}$	$M_{w\beta}$	m_E
M1	3.12-i1.81	15.7-i0.37	0.60+i0.04	0.13+i0.72	-0.89-i0.11	-0.45+i0.07	7
M2	2.18-i0.17	8.92+i0.14	0.92+i0.04	-0.02-i0.38	-0.29-i0.13	-0.69+i0.23	6.5
M3	7.33-i0.85	6.59+i0.49	1.42+i0.03	0.51+i3.05	0.52-i0.41	-0.70-i0.58	12
M4	9.39-i0.74	7.92-i0.06	2.70+i0.14	-0.21+i2.84	-0.88-i0.73	-0.89-i0.53	18
M5	13.1+i0.14	12.7+i0.25	8.12-i0.06	-0.16-i0.13	-0.38-i0.11	0.38+i0.03	15

Table 2. Shown are the input mass parameters of the benchmark models M1-M5 along with the mass of the new charged doublet state m_E . All masses are given in units 100 GeV. Note that the mass of the new adjoint state ω_D equals with the Majorana mass $m_{wD} = M_{ww}$.

Kamiokande limits, that concern the WIMPs that accumulate in the core of the Sun and then annihilate to W -bosons, have some constraining power in the mass region $m_{DM} \lesssim 200$ GeV. At first sight it seems that the latest Super-Kamiokande results, concerning WIMPs that annihilate into tau leptons, also have some constraining power. Note however, that the points above the Super-Kamiokande $\tau^+\tau^-$ -line in Fig. 2 are *not* excluded. This is because the Super-Kamiokande constraint assumes that WIMPs annihilate into taus with a branching ratio $\text{Br}_{\tau\tau} = 1$. Here in general, and in the accepted models falling above the Super-Kamiokande constraint in particular, the branching ratio to taus is much less than one. For DM masses below W^+W^- threshold our WIMPs annihilate dominantly to $b\bar{b}$ -channel, and the $\tau^+\tau^-$ branching is only ~ 0.05 (for branching ratios in specific benchmark models see table 3). Furthermore, this ratio only decreases once other annihilation channels open for $m_{DM} \geq m_W$. Due to these small annihilation branching fractions, the Super-Kamiokande limits are currently very little constraining.

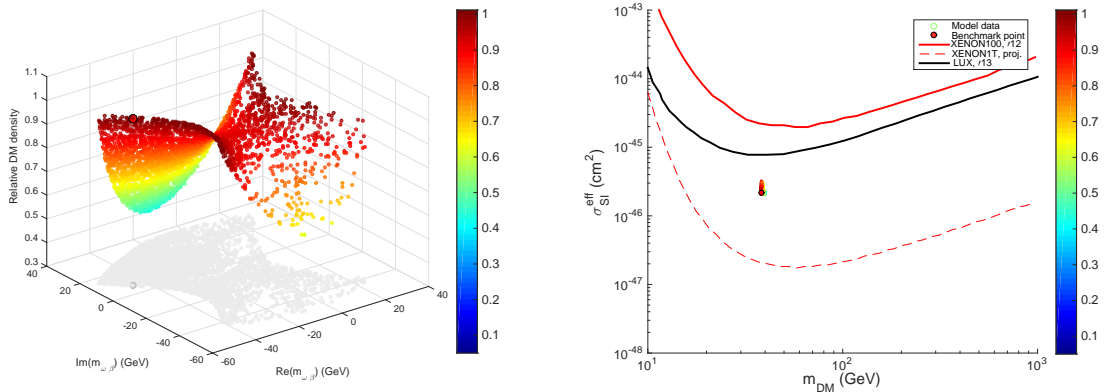


Figure 5. Left: shown is the result of a restricted MCMC-scan in the complex mass parameter $m_{w\beta}$ around the benchmark point M1 in Table 2. Light gray dots show the projections of the points to the complex mass plane. Right: the projection of these points in $(m_{DM}, \sigma_{SI}^{\text{eff}})$ -plane.

4.2 Benchmark models

A generic MCMC scan over the entire prior range gives a good idea of the constraining power of the different observations. However, because of the high-dimensionality of the parameter space, such scans do not reveal the finer details of how acceptable models are distributed. In particular it appears that there are but a few sets of parameters that give $f_{\text{rel}} \approx 1$. For this reason we selected five benchmark points from the accepted MCMC data sets and made new runs with restricted priors in their neighborhoods. The selected models are labelled as M1-M5 and shown by large red dots in the scatter plots 2-6 and 8. The corresponding central parameter values are given in table 2. In table 3 we show the ensuing DM mass, relative DM-abundance, precision electroweak parameters S and T , the effective WIMP-nucleon cross section σ_{SI}^{eff} , the tau-branching ratio $\text{Br}_{\tau\tau}$, the contribution to Z -width and the invisible Higgs decay fraction R_I for these models. Note that models 2-5 have large and positive S and T -parameters. This is a generic feature in our model, due to the fact that the precision variables, and S in particular, get a large positive contribution from technicolor fields (see table 1). As is evident from figure 4, a strict bound on the S -parameter $S < 0.1$ could rule the model out completely. However, the contributions from flavor extensions are subtle and may quantitatively affect the analysis [66, 67]. We give no values for S and T for model 1, because our precision data analysis [16] is not applicable for $m_{DM} < M_Z/2$. However, we expect that the strongest bound comes from the Z -decay width in this region.

In the left panel of figure 5 we show a scan of parameters around the benchmark Model 1. We fixed all parameters as given in table 2 except $M_{w\beta}$, which was allowed to vary freely in an MCMC scan starting from the benchmark value. This scan reveals a continuous, but constrained domain of parameters giving a right, or very closely right DM abundance. In the right panel we show how these points are all tightly concentrated in the the DM mass-effective SI-cross section diagram. This example shows that the apparent deficit of points with $f_{\text{rel}} \approx 1$ in Figs. 2-4 may give a too pessimistic idea of the density of acceptable models. Figure 6 shows a result of an MCMC-run around the benchmark model 3, fixing all parameters but the complex mass M_{NN} . First, we observe that f_{rel} is almost independent of M_{NN} . This is

	m_{DM}	f_{rel}	S	T	$\sigma_{\text{SI}}^{\text{eff}}$	$\text{Br}_{\tau\tau}$	δ_Z	R_I
M1	38	1.00	-	-	2.2×10^{-46}	0.051	0.0008	0.12
M2	84	0.96	0.11	0.13	1.7×10^{-46}	0.0012	-	-
M3	137	1.01	0.18	0.14	1.3×10^{-45}	7.7×10^{-5}	-	-
M4	246	1.01	0.16	0.15	9.1×10^{-46}	1.3×10^{-5}	-	-
M5	806	0.87	0.22	0.19	3.7×10^{-45}	9.9×10^{-7}	-	-

Table 3. Shown are the values of DM mass m_{DM} , relative relic density f_{rel} , precision S and T parameters, the effective cross section $\sigma_{\text{SI}}^{\text{eff}}$, the contribution to Z -width δ_Z and the invisible Higgs decay fraction R_I for the benchmark models. A dash indicates that the bound is not relevant for the model in question.

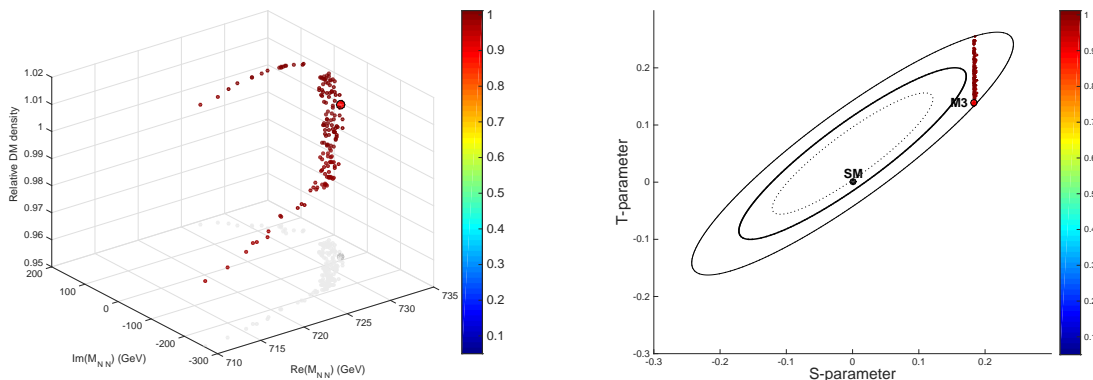


Figure 6. Left: shown is the result of a restricted MCMC-scan in the complex mass parameter m_{NN} around the benchmark point M3 in Table 2. Right: the projection of these points in (S, T) -plane.

because DM is always mostly β -like and so its mass and couplings do not depend much on the NN-entry of the mass matrix. Second, only a thin line of acceptable solutions are found. The reason for this is the T -parameter, which gets a large contribution from the doublet-like states, and the contribution from the N -like neutral state must accurately cancel the contribution from the charged E -state [22]. For a fixed m_E this works only for a very narrow range in the mass of the N -like state, which is essentially set by M_{NN} . This explains why points with $f_{\text{rel}} \approx 1$ are relatively sparsely distributed in the generic MCMC plots: our full parameter space has many dimensions (thirteen) and good models are forced to lie on narrow low-dimensional strips, which are hard to locate in a full parameter space scan. However, when good solutions are found, one in general finds continuous sheets of acceptable solutions in their immediate neighborhood.

5 Additional bounds: Higgs to $\gamma\gamma$ and a light composite scalar

As already emphasized, our generic DM setting provides a very attractive solution for the particle dark matter problem, the hierarchy problem and the gauge unification. However, before concluding, we still need to discuss two additional constraints. First, the bound on higgs decay to two photons and second, the lightness of the higgs mass in the effective field

theory picture underlying the model. We find that both issues can be addressed within the strongly interacting sector of the model and do not have consequences for the DM physics. Even though these bounds are of no concern for our main results on dark matter, we discuss them for the benefit of the overall consistency of the model. A reader not interested in these details may skip directly to the conclusions.

5.1 Higgs to $\gamma\gamma$

There are a number of new particles in our model, which can influence the Higgs boson decay widths. As we have already discussed, if our DM is light enough, $m_{\text{DM}} < m_h/2$, it opens up a new invisible Higgs decay channel, which would change the predicted higgs branching ratios. In addition, all new charged particles contribute to Higgs decays to two photons via loop corrections.

The contribution from new TC singlets, the new heavy electron E^\pm and the new charged w_D^\pm state nested in the SU(2) triplet, are easy to compute. The sector which is not singlet under TC is more model dependent. To estimate this effect we consider the contributions of heavy massive resonances within the sigma model-like effective theory describing the Higgs sector at low energies. The loop corrections induced by vectors to $\gamma\gamma$ -amplitude are much larger than those from scalars with a similar coupling strength, and so vector resonances may easily dominate the effective $H\gamma\gamma$ coupling. Concretely, we consider a simple setup with one extra charged vector resonance, described as a new effective massive W' -boson. The relevant effective Lagrangian then is

$$\begin{aligned} \mathcal{L}_{\text{eff,H}} = & \frac{2m_W^2 c_W}{v} h W_\mu^- W^{+\mu} + \frac{m_Z^2 c_Z}{v} h Z_\mu Z^\mu \\ & - \sum_f \frac{m_f c_f}{v} h \bar{f} f + \frac{2m_{W'}^2 c_{W'}}{v} h W_\mu'^- W'^{+\mu}. \end{aligned} \quad (5.1)$$

The sum f runs over the charged SM fermions and the new charged techni-singlet fermions. In practice these are the top quark, the new heavy electron E and the w^\pm states. The effective fermion and EW vector boson couplings of the Higgs are denoted by c_f and c_W so that for SM we have $c_f = c_W = 1$. In our model $c_E = 1$ and $c_{w^\pm} = 2$, while the couplings to the top quark and W -bosons must be inferred from the LHC data. Generally, on the basis of extrapolating from QCD and explicit model calculations [67, 68], it is expected that in this type of a model $c_W = c_Z \approx 1$ and $c_t \approx 1$ which is also confirmed by fits to the LHC data [68].⁶

For simplicity and for less model dependence we have written the Lagrangian in terms of mass eigenstates. We also neglected the mixing of W -and W' -bosons, which in general could lead to a correlation between W -and W' -boson couplings. With these assumptions all non-conventional effects due to charged resonances are modelled by the coupling factor $c_{W'}$.

The full 1-loop decay width of Higgs to two photons is

$$\Gamma_{\gamma\gamma} = \frac{m_H^3}{4\pi v} (g_{H\gamma\gamma})^2, \quad (5.2)$$

⁶Note that the Higgs coupling to gluons is SM-like, since we assume that all the new particles coupling with the Higgs are color singlets.

where the effective coupling is given by

$$g_{H\gamma\gamma} = \frac{\alpha}{8\pi} \left| \sum_f c_f N_c^f Q_f^2 F_{1/2}(\tau_f) + c_W F_1(\tau_W) + c_{W'} F_1(\tau_{W'}) \right|. \quad (5.3)$$

The color factors of non-standard model fields are $N_c^E = N_c^{w^\pm} = 1$ and the loop factors $F_i(\tau_j)$ for fermions ($i = 1/2$) and for vector bosons ($i = 1$) are standard,

$$\begin{aligned} F_{1/2}(\tau_f) &\equiv -2\tau_f [1 + (1 - \tau_f)f(\tau_f)], \\ F_1(\tau_W) &\equiv 2 + 3\tau_W + 3\tau_W(2 - \tau_W)f(\tau_W), \end{aligned} \quad (5.4)$$

where

$$f(\tau_j) \equiv \begin{cases} \arcsin^2 \frac{1}{\sqrt{\tau_j}} & \text{if } \tau_j \geq 1 \\ -\frac{1}{4} \left[\log \frac{1 + \sqrt{1 - \tau_j}}{1 - \sqrt{1 - \tau_j}} - i\pi \right]^2 & \text{if } \tau_j < 1 \end{cases} \quad (5.5)$$

and $\tau_j \equiv 4m_j^2/m_H^2$. For τ_j larger than unity, the loop-factors quickly reach the asymptotic values $F_{1/2}(\infty) = -4/3$ and $F_1(\infty) = 7$. Using the asymptotic value is a good approximation for all new fermions and even for the top quark the relative error of this approximation is about three per cent. Consequently, since the techni-resonances are expected to be in $\mathcal{O}(\text{TeV})$ mass range, the exact value of the W' mass is not relevant and $F_1(m_{W'}) \approx 7$.

The effective coupling $c_{W'}$, can now be constrained by existing bounds on the ratio of the Higgs branching fractions to two photons ⁷, *i.e.* $\text{BR}_{\gamma\gamma}/\text{BR}_{\gamma\gamma}^{\text{SM}}$. We extracted a 2σ -limit for this quantity from the left panel of Fig. 5 of ref. [53]. The experimental bound is then converted to a constraint on $c_{W'}$ assuming no invisible decay channels. The result is shown in Fig. 7. The rather loose bound $0.52 \lesssim c_{W'} \lesssim 0.85$ indicates that our model can be made consistent with the data by rather modest and reasonable assumptions about the structure of the effective low-energy theory.

Another possibility would be to include the TC dynamics by considering the elementary fields, *i.e.* charged techniquarks, inside the loop and interacting with the TC-Higgs. We have checked, adapting the results of [68] to our SM-like hypercharge convention, that that this leads to quantitatively similar and consistent results with the effective model approach we have detailed here.

5.2 Dynamical Higgs boson mass scale

Then we discuss how a light composite Higgs relates to the intrinsic dynamical scale of the model. The traditional expectation of a heavy scalar resonance assumes TC dynamics in isolation. It is known that couplings with the EW gauge currents and extended flavour sectors, in particular the top quark, affect this conclusion [66, 67, 70]. In addition, our model contains several new heavy fields that couple to the Higgs and contribute to its vacuum polarization. We estimate this effect quantitatively by use of a perturbative one-loop approximation. As usual, we induce a cut-off Λ to evaluate the relevant 1-loop integrals. However, since Λ is not very large here, we keep nonzero masses for the heaviest particles in the loops. This

⁷Recent results from Atlas collaboration [69] favor a slightly larger $\gamma\gamma$ -branching fraction, $\text{BR}_{\gamma\gamma}/\text{BR}_{\gamma\gamma}^{\text{SM}} > 1$. As is evident from Fig. 7, this situation is naturally realized in our model.

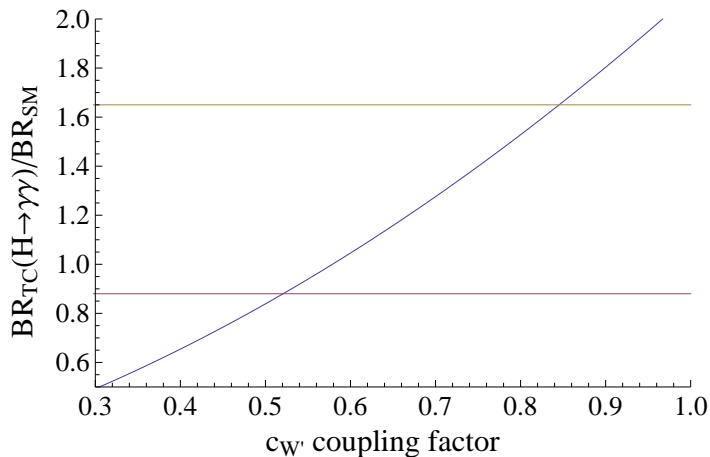


Figure 7. Shown is the 2σ -limit for the coupling factor $c_{W'}$. The allowed region is between the horizontal lines. The factor $c_{W'}$ is the effective coupling between techni-vector resonance and the techni-Higgs.

procedure gives:

$$\begin{aligned}
m_H^2 = & (m_H^{\text{TC}})^2 + [6m_W^2 + 3m_Z^2 - 12m_t^2] \frac{\Lambda^2}{16\pi^2 v^2} \\
& - 4 \sum_i f_i m_i^2 \frac{\Lambda^2}{16\pi^2 v^2} \left(1 - \frac{m_i^2}{\Lambda^2} \log \frac{\Lambda^2}{m_i^2} \right). \tag{5.6}
\end{aligned}$$

Here m_H^{TC} is the intrinsic dynamical TC Higgs boson mass, which we attempt to estimate. The cut-off dependent part in the first line includes corrections from the relevant SM particles and the sum in the second line the corrections from the new heavy fermions. These include the charged fermions E and ω^\pm with factors $f_E = 1$ and $f_{\omega^\pm} = 4$ and the two heaviest neutral Majorana fermions with a factor $f_{\chi_i} = 4$ for each⁸. We approximate the masses of the neutral states by M_{NN} and M_{ww} , which is a reasonable approximation, as the Dirac mass terms are typically small compared to the diagonal Majorana masses in the original WIMP mass matrix. Thus the mixings are small and finally the contribution from the relatively light WIMP is suppressed compared to the other two Majorana states.

The cut-off is provided by the TC-scale, which here, consistently with the unification: $\Lambda \sim \Lambda_{\text{TC}} \approx 3$ TeV (see Sec. 3). For concreteness we used $\Lambda = 1.5$ TeV. We can now turn Eq. (5.6) around, setting $m_H = 125$ GeV and solve it for the dynamical Higgs mass m_H^{TC} for all models in our data set. The result is shown in Fig. 8. Models with $2m_{\text{DM}} > M_Z$ give $m_H^{\text{TC}} \sim 1$ -2 TeV. This is of the right order of magnitude, since one would expect that in a conventional technicolor model $m_H^{\text{TC}} < 4\pi v \approx \text{few TeV}$. For models with $m_{\text{DM}} < M_Z/2$ the small mixing approximation made in using Eq. (5.6) breaks down and the results for m_H^{TC} cannot be trusted. Anyway, these arguments strongly suggest that the Higgs boson can indeed be naturally light in our model.

⁸The factor $f_i = 4$ follows from the expansion of the Higgs interaction term $(1 + h/v)^2 \rightarrow 2h/v$. This factor of two in the coupling gives the factor of four in the loop.

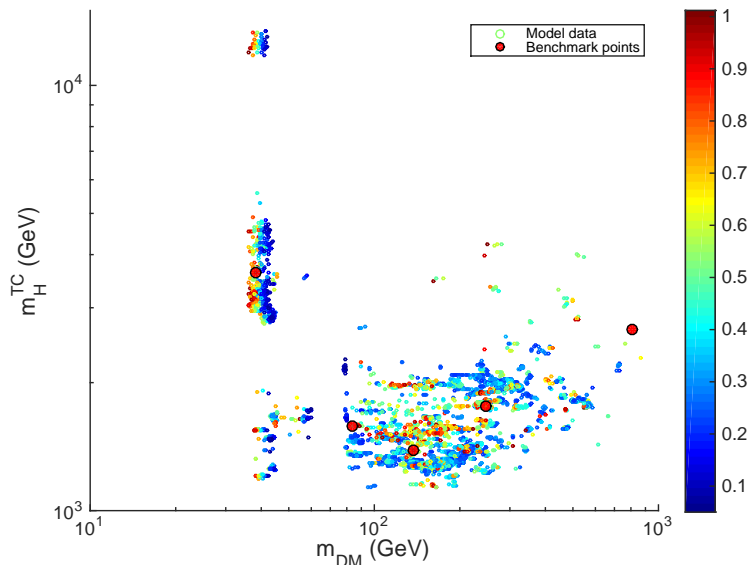


Figure 8. Scatter of the one-loop estimate for the intrinsic TC Higgs mass m_H^{TC} for our accepted models. The colour coding again indicates the relative DM density.

6 Conclusions

We have analysed a model for dynamical symmetry breaking, dark matter and gauge coupling unification in light of the most recent observational and experimental data. The model setting is nontrivial, but very tightly constrained theoretically. Since the model does not contain any light fundamental scalars, there is no hierarchy problem. We have shown how the model gives rise to perfect 1-loop unification of all gauge couplings, including the new technicolor interaction, at a common unification scale $M_U = 2.2 \times 10^{15}$ GeV and the unified coupling $\alpha_U \approx 0.0304$. Moreover, unification determines the scale of the 1-loop IR-pole of the TC-coupling $\Lambda_{\text{TC}}^{1\text{-loop}} \approx 340$ GeV. By the QCD analogue, this is consistent with the naive expectation of the the TC interactions becoming strong around the scale $\Lambda_{\text{TC}} \sim \mathcal{O}(\text{TeV})$. Thus unification is not only possible, but it actually supports the existence of a TeV-scale strongly interacting dynamical sector.

The essential part of the spectrum are the fermion fields transforming under adjoint representations of the gauge group. In terms of their quantum numbers these fermions are identical to the gauginos which arise in supersymmetric setting. Hence, it is natural to entertain the thought that the model is a low energy realization of a supersymmetric theory. The existence of a strongly coupled sector responsible for the electroweak symmetry breaking naturally decouples supersymmetry breaking from the electroweak physics, hence removing the little hierarchy problem [71–73]. Consequently the scalar superpartners can all be very heavy with masses around or above the unification scale M_U . More detailed model building and investigation of resulting phenomenology provide interesting further research prospects. It would be also desirable to have more detailed theory which explains the effective scalar-fermion couplings in our low energy lagrangian and the emergence of fermion mass patterns. The details of underlying flavor physics likely require an extensions of the technicolor gauge

dynamics.

In this paper our main analysis concerned the dark matter sector of the model. The dark matter candidate arises from mixing of three neutral fields: one gauge singlet, a neutral member of an $SU(2)$ -doublet and an $SU(2)$ triplet. The stability of the lightest of these fields is guaranteed by a discrete Z_2 -symmetry. The most essential parameters for the dark matter in model are the entries in the effective mixing mass matrix of these neutral states. We performed a generic MCMC scan of the model parameter space constraining the model by the most recent bounds following from the accelerators as well as direct and indirect DM-searches.

We also introduced several explicit benchmark cases to illustrate typical features of viable models and performed limited range MCMC runs in the neighborhood of the benchmark points to study the allowed phase space in more detail. We found that there are large continuous regions of parameters for which the model can provide a naturally stable DM particle with a mass in the range $m_{\text{DM}} \sim 30 - 800$ GeV.

We conclude that the model is viable in light of existing data from collider experiments and cosmological and astrophysical observations. However, future experiments have excellent possibilities to probe the model further: Most of the available parameter space is within the reach of the next generation of DM search experiments. Also a significant shift of the observed precision electroweak parameters towards their SM-values, in particular of the Peskin-Takeuchi S -parameter, could rule out the model as a source for DM. Finally, the experimental results on the proton decay will constrain the unification aspects of the model. Of course the interesting possibility is that one or the other of these observations would provide the first evidence of particles compatible with the low-energy spectrum predicted by the model.

Acknowledgements

We acknowledge the financial support from the Academy of Finland, projects 278722 and 267842.

References

- [1] **ATLAS Collaboration**, G. Aad et al., *Observation of a new particle in the search for the Standard Model Higgs boson with the ATLAS detector at the LHC*, *Phys.Lett.* **B716** (2012) 1–29, [[arXiv:1207.7214](#)].
- [2] **CMS Collaboration** Collaboration, S. Chatrchyan et al., *Observation of a new boson at a mass of 125 GeV with the CMS experiment at the LHC*, *Phys.Lett.* **B716** (2012) 30–61, [[arXiv:1207.7235](#)].
- [3] J. McDonald, *Gauge singlet scalars as cold dark matter*, *Phys.Rev.* **D50** (1994) 3637–3649, [[hep-ph/0702143](#)].
- [4] J. McDonald, *Thermally generated gauge singlet scalars as selfinteracting dark matter*, *Phys.Rev.Lett.* **88** (2002) 091304, [[hep-ph/0106249](#)].
- [5] C. Burgess, M. Pospelov, and T. ter Veldhuis, *The Minimal model of nonbaryonic dark matter: A Singlet scalar*, *Nucl.Phys.* **B619** (2001) 709–728, [[hep-ph/0011335](#)].
- [6] L. Lopez Honorez, E. Nezri, J. F. Oliver, and M. H. Tytgat, *The Inert Doublet Model: An Archetype for Dark Matter*, *JCAP* **0702** (2007) 028, [[hep-ph/0612275](#)].

- [7] J. M. Cline, K. Kainulainen, P. Scott, and C. Weniger, *Update on scalar singlet dark matter*, *Phys.Rev.* **D88** (2013) 055025, [[arXiv:1306.4710](#)].
- [8] J. M. Cline and K. Kainulainen, *Improved Electroweak Phase Transition with Subdominant Inert Doublet Dark Matter*, *Phys.Rev.* **D87** (2013) 071701, [[arXiv:1302.2614](#)].
- [9] J. M. Cline and K. Kainulainen, *Electroweak baryogenesis and dark matter from a singlet Higgs*, *JCAP* **1301** (2013) 012, [[arXiv:1210.4196](#)].
- [10] T. Alanne, K. Tuominen, and V. Vaskonen, *Strong phase transition, dark matter and vacuum stability from simple hidden sectors*, *Nucl.Phys.* **B889** (2014) 692–711, [[arXiv:1407.0688](#)].
- [11] B. Holdom, *Technicolor*, *Phys.Lett.* **B150** (1985) 301.
- [12] K. Yamawaki, M. Bando, and K.-i. Matumoto, *Scale Invariant Technicolor Model and a Technidilaton*, *Phys.Rev.Lett.* **56** (1986) 1335.
- [13] F. Sannino and K. Tuominen, *Orientifold theory dynamics and symmetry breaking*, *Phys.Rev.* **D71** (2005) 051901, [[hep-ph/0405209](#)].
- [14] D. D. Dietrich, F. Sannino, and K. Tuominen, *Light composite Higgs from higher representations versus electroweak precision measurements: Predictions for CERN LHC*, *Phys.Rev.* **D72** (2005) 055001, [[hep-ph/0505059](#)].
- [15] K. Kainulainen, K. Tuominen, and J. Virkajarvi, *Naturalness, unification and dark matter*, *Phys.Rev.* **D82** (2010) 043511, [[arXiv:1001.4936](#)].
- [16] K. Kainulainen, K. Tuominen, and J. Virkajarvi, *Dark matter from unification*, *JCAP* **1310** (2013) 036, [[arXiv:1307.1546](#)].
- [17] S. B. Gudnason, T. A. Rytto, and F. Sannino, *Gauge coupling unification via a novel technicolor model*, *Phys.Rev.* **D76** (2007) 015005, [[hep-ph/0612230](#)].
- [18] S. Nussinov, *TECHNOCOSMOLOGY: COULD A TECHNIBARYON EXCESS PROVIDE A 'NATURAL' MISSING MASS CANDIDATE?*, *Phys.Lett.* **B165** (1985) 55.
- [19] R. S. Chivukula and T. P. Walker, *TECHNICOLOR COSMOLOGY*, *Nucl.Phys.* **B329** (1990) 445.
- [20] S. M. Barr, R. S. Chivukula, and E. Farhi, *Electroweak Fermion Number Violation and the Production of Stable Particles in the Early Universe*, *Phys.Lett.* **B241** (1990) 387–391.
- [21] S. B. Gudnason, C. Kouvaris, and F. Sannino, *Dark Matter from new Technicolor Theories*, *Phys.Rev.* **D74** (2006) 095008, [[hep-ph/0608055](#)].
- [22] K. Kainulainen, K. Tuominen, and J. Virkajarvi, *The WIMP of a Minimal Technicolor Theory*, *Phys.Rev.* **D75** (2007) 085003, [[hep-ph/0612247](#)].
- [23] C. Kouvaris, *Dark Majorana Particles from the Minimal Walking Technicolor*, *Phys.Rev.* **D76** (2007) 015011, [[hep-ph/0703266](#)].
- [24] M. Y. Khlopov and C. Kouvaris, *Strong Interactive Massive Particles from a Strong Coupled Theory*, *Phys.Rev.* **D77** (2008) 065002, [[arXiv:0710.2189](#)].
- [25] M. Y. Khlopov and C. Kouvaris, *Composite dark matter from a model with composite Higgs boson*, *Phys.Rev.* **D78** (2008) 065040, [[arXiv:0806.1191](#)].
- [26] T. A. Rytto and F. Sannino, *Ultra Minimal Technicolor and its Dark Matter TIMP*, *Phys.Rev.* **D78** (2008) 115010, [[arXiv:0809.0713](#)].
- [27] R. Foadi, M. T. Frandsen, and F. Sannino, *Technicolor Dark Matter*, *Phys.Rev.* **D80** (2009) 037702, [[arXiv:0812.3406](#)].
- [28] K. Kainulainen, J. Virkajarvi, and K. Tuominen, *Superweakly interacting dark matter from the Minimal Walking Technicolor*, *JCAP* **1002** (2010) 029, [[arXiv:0912.2295](#)].

- [29] T. Hapola, M. Jarvinen, C. Kouvaris, P. Panci, and J. Virkajarvi, *Constraints on Majorana Dark Matter from a Fourth Lepton Family*, *JCAP* **1402** (2014) 050, [[arXiv:1309.6326](#)].
- [30] T. A. Ryttov and F. Sannino, *Conformal House*, *Int.J.Mod.Phys.* **A25** (2010) 4603–4621, [[arXiv:0906.0307](#)].
- [31] K.-i. Kondo, H. Mino, and K. Yamawaki, *Critical Line and Dilaton in Scale Invariant QED*, *Phys.Rev.* **D39** (1989) 2430.
- [32] T. Appelquist, M. Soldate, T. Takeuchi, and L. Wijewardhana, *Effective four-fermion interactions and chiral symmetry breaking in TeV physics: proceedings, G. Domokos, S. Kovesi-Domokos and N.J Teaneck eds.*, *World Scientific* (1988).
- [33] H. S. Fukano and F. Sannino, *Conformal Window of Gauge Theories with Four-Fermion Interactions and Ideal Walking*, *Phys.Rev.* **D82** (2010) 035021, [[arXiv:1005.3340](#)].
- [34] **Particle Data Group** Collaboration, K. Olive et al., *Review of Particle Physics*, *Chin.Phys.* **C38** (2014) 090001.
- [35] L.-F. Li and F. Wu, *Coupling constant unification in extensions of standard model*, *Int.J.Mod.Phys.* **A19** (2004) 3217–3224, [[hep-ph/0304238](#)].
- [36] G. G. Ross, *GRAND UNIFIED THEORIES*, *Benjamin Cummings* (1984).
- [37] G. Giudice and A. Romanino, *Split supersymmetry*, *Nucl.Phys.* **B699** (2004) 65–89, [[hep-ph/0406088](#)].
- [38] **JLQCD** Collaboration, S. Aoki et al., *Nucleon decay matrix elements from lattice QCD*, *Phys.Rev.* **D62** (2000) 014506, [[hep-lat/9911026](#)].
- [39] **RBC-UKQCD** Collaboration, Y. Aoki et al., *Proton lifetime bounds from chirally symmetric lattice QCD*, *Phys.Rev.* **D78** (2008) 054505, [[arXiv:0806.1031](#)].
- [40] Y. Aoki, E. Shintani, and A. Soni, *Proton decay matrix elements on the lattice*, *Phys.Rev.* **D89** (2014), no. 1 014505, [[arXiv:1304.7424](#)].
- [41] **Planck** Collaboration, P. Ade et al., *Planck 2015 results. XIII. Cosmological parameters*, [[arXiv:1502.0158](#)].
- [42] **XENON100** Collaboration Collaboration, E. Aprile et al., *Dark Matter Results from 225 Live Days of XENON100 Data*, *Phys.Rev.Lett.* **109** (2012) 181301, [[arXiv:1207.5988](#)].
- [43] **LUX** Collaboration Collaboration, D. Akerib et al., *First results from the LUX dark matter experiment at the Sanford Underground Research Facility*, *Phys.Rev.Lett.* **112** (2014) 091303, [[arXiv:1310.8214](#)].
- [44] **PICO** Collaboration, C. Amole et al., *Dark Matter Search Results from the PICO-2L C₃F₈ Bubble Chamber*, *Phys. Rev. Lett.* **114** (2015) 231302, [[arXiv:1503.0000](#)].
- [45] **IceCube** Collaboration Collaboration, R. Abbasi et al., *Multi-year search for dark matter annihilations in the Sun with the AMANDA-II and IceCube detectors*, *Phys.Rev.* **D85** (2012) 042002, [[arXiv:1112.1840](#)].
- [46] **IceCube** collaboration Collaboration, M. Aartsen et al., *Search for dark matter annihilations in the Sun with the 79-string IceCube detector*, *Phys.Rev.Lett.* **110** (2013) 131302, [[arXiv:1212.4097](#)].
- [47] **Super-Kamiokande** Collaboration, K. Choi et al., *Search for neutrinos from annihilation of captured low-mass dark matter particles in the Sun by Super-Kamiokande*, *Phys.Rev.Lett.* **114** (2015), no. 14 141301, [[arXiv:1503.0485](#)].
- [48] **Super-Kamiokande** Collaboration Collaboration, T. Tanaka et al., *An Indirect Search for WIMPs in the Sun using 3109.6 days of upward-going muons in Super-Kamiokande*, *Astrophys.J.* **742** (2011) 78, [[arXiv:1108.3384](#)].

- [49] M. E. Peskin and T. Takeuchi, *A New constraint on a strongly interacting Higgs sector*, *Phys.Rev.Lett.* **65** (1990) 964–967.
- [50] **Particle Data Group** Collaboration, J. Beringer et al., *Review of Particle Physics (RPP)*, *Phys.Rev.* **D86** (2012) 010001.
- [51] P. P. Giardino, K. Kannike, M. Raidal, and A. Strumia, *Is the resonance at 125 GeV the Higgs boson?*, *Phys.Lett.* **B718** (2012) 469–474, [[arXiv:1207.1347](#)].
- [52] B. A. Dobrescu and J. D. Lykken, *Coupling spans of the Higgs-like boson*, *JHEP* **1302** (2013) 073, [[arXiv:1210.3342](#)].
- [53] P. P. Giardino, K. Kannike, I. Masina, M. Raidal, and A. Strumia, *The universal Higgs fit*, *JHEP* **1405** (2014) 046, [[arXiv:1303.3570](#)].
- [54] **XENON1T** Collaboration, E. Aprile, *The XENON1T Dark Matter Search Experiment*, *Springer Proc. Phys.* **148** (2013) 93–96, [[arXiv:1206.6288](#)].
- [55] **IceCube collaboration** Collaboration, R. Abbasi et al., *Search for Neutrinos from Annihilating Dark Matter in the Direction of the Galactic Center with the 40-String IceCube Neutrino Observatory*, [arXiv:1210.3557](#).
- [56] F.-F. Lee, G.-L. Lin, and Y.-L. S. Tsai, *Sensitivities of IceCube DeepCore Detector to Signatures of Low-Mass Dark Matter in the Galactic Halo*, *Phys.Rev.* **D87** (2013) 025003, [[arXiv:1209.6226](#)].
- [57] **IceCube** Collaboration, M. G. Aartsen et al., *The IceCube Neutrino Observatory Part IV: Searches for Dark Matter and Exotic Particles*, [arXiv:1309.7007](#).
- [58] M. R. Buckley, E. Charles, J. M. Gaskins, A. M. Brooks, A. Drlica-Wagner, et al., *Search for Gamma-ray Emission from Dark Matter Annihilation in the Large Magellanic Cloud with the Fermi Large Area Telescope*, *Phys.Rev.D* (2015) [[arXiv:1502.0102](#)].
- [59] **Fermi-LAT** Collaboration, M. Ackermann et al., *Limits on Dark Matter Annihilation Signals from the Fermi LAT 4-year Measurement of the Isotropic Gamma-Ray Background*, [arXiv:1501.0546](#).
- [60] **LAT collaboration** Collaboration, M. Ackermann et al., *Constraints on the Galactic Halo Dark Matter from Fermi-LAT Diffuse Measurements*, *Astrophys.J.* **761** (2012) 91, [[arXiv:1205.6474](#)].
- [61] **LAT Collaboration** Collaboration, M. Ackermann et al., *Fermi LAT Search for Dark Matter in Gamma-ray Lines and the Inclusive Photon Spectrum*, *Phys.Rev.* **D86** (2012) 022002, [[arXiv:1205.2739](#)].
- [62] **Veritas Collaboration** Collaboration, T. Arlen et al., *Constraints on Cosmic Rays, Magnetic Fields, and Dark Matter from Gamma-Ray Observations of the Coma Cluster of Galaxies with VERITAS and Fermi*, *Astrophys.J.* **757** (2012) 123, [[arXiv:1208.0676](#)].
- [63] **Fermi-LAT** Collaboration, M. Ackermann et al., *Searching for Dark Matter Annihilation from Milky Way Dwarf Spheroidal Galaxies with Six Years of Fermi-LAT Data*, [arXiv:1503.0264](#).
- [64] G. Giesen, M. Boudaud, Y. Genolini, V. Poulin, M. Cirelli, et al., *AMS-02 antiprotons, at last! Secondary astrophysical component and immediate implications for Dark Matter*, [arXiv:1504.0427](#).
- [65] AMS-02 Collaboration, “Talks at the ‘AMS Days at CERN’.” <http://indico.cern.ch/event/381134/overview>, 2015. [15-17 April].
- [66] S. Di Chiara, R. Foadi, and K. Tuominen, *125 GeV Higgs from a chiral techniquark model*, *Phys.Rev.* **D90** (2014), no. 11 115016, [[arXiv:1405.7154](#)].
- [67] S. Di Chiara, R. Foadi, K. Tuominen, and S. Tahtinen, *Dynamical Origin of the Electroweak Scale and the 125 GeV Scalar*, [arXiv:1412.7835](#).

- [68] A. Belyaev, M. S. Brown, R. Foadi, and M. T. Frandsen, *The Technicolor Higgs in the Light of LHC Data*, *Phys. Rev.* **D90** (2014) 035012, [[arXiv:1309.2097](#)].
- [69] **ATLAS** Collaboration, G. Aad et al., *Measurements of the Total and Differential Higgs Boson Production Cross Sections Combining the $H \rightarrow \gamma\gamma$ and $H \rightarrow ZZ^* \rightarrow 4\ell$ Decay Channels at $\sqrt{s} = 8$ TeV with the ATLAS Detector*, [arXiv:1504.0583](#).
- [70] R. Foadi, M. T. Frandsen, and F. Sannino, *125 GeV Higgs boson from a not so light technicolor scalar*, *Phys. Rev.* **D87** (2013) 095001, [[arXiv:1211.1083](#)].
- [71] M. Dine, W. Fischler, and M. Srednicki, *Supersymmetric Technicolor*, *Nucl.Phys.* **B189** (1981) 575–593.
- [72] M. Antola, S. Di Chiara, F. Sannino, and K. Tuominen, *Supersymmetric Extension of Technicolor & Fermion Mass Generation*, *Nucl.Phys.* **B864** (2012) 664–693, [[arXiv:1111.1009](#)].
- [73] M. Antola, S. Di Chiara, and K. Tuominen, *Ultraviolet Complete Technicolor and Higgs Physics at LHC*, [arXiv:1307.4755](#).